Supporting Information

Binding of GS-461203 and its Halogen Derivatives to HCV Genotype 2a RNA Polymerase Drug Resistance Mutants

Muhammad Arba[1*], Setyanto Tri Wahyudi[2], Muhammad Sulaiman Zubair[3], Dylan Brunt[4], Mursalin Singh[4] and Chun Wu[4*]

[1] *Department of Pharmacy, Faculty of Pharmacy, Universitas Halu Oleo, Kendari 93232, Indonesia*; muh.arba@uho.ac.id
[2] *Department of Physics, IPB University, Bogor 16680, Indonesia*
[3] *Department of Pharmacy, Faculty of Science, Tadulako University, Palu 94118, Indonesia*
[4] *Department of Molecular & Cellular Biosciences, College of Science and Mathematics, Rowan University, Glassboro, New Jersey 08028, United States; wuc@rowan.edu*
* Correspondence: muh.arba@uho.ac.id (MA); wuc@rowan.edu (CW)

Table caption

Table S1. The binding energies calculated for the last 50 ns of S282T system.
Table S2. The binding energies calculated for the last 50 ns of each individual trajectory.

Figure caption
Figure. S1 The docked and experimental poses of GS-461203.
Figure S2. The RMSD of Protein Cα and ligand in WT run-1 (A), WT run-2 (B); T179A-run1 (C), T179A run-2 (D), S282T run-1 (E), S282T-run2 (F), M289L run-1 (G), and M289L run-2.
Figure S3. The histogram diagram and the fraction of the simulation for each type of interaction showing all residues interacting with GS-461203 (**A:** WT-GS-461203; **B:** T179A-GS-461203; **C:** S282T-GS-461203; **D:** M289L-GS-461203) recorded during MDS.
Figure S4. Protein-Ligand Interactions **A:** WT-GS-461203-run1; **B:** WT-GS-461203-run3; **C:** T179A-GS-461203-run3; **D:** T179A-GS-461203-run4; **E:** S282T-GS-461203-run1; **F:** S282T-GS-461203-run2; **G:** M289L-GS-461203-run1; **H:** M289L-GS-461203-run3, recorded during MDS. Left: the histogram diagram and the fraction of the simulation for each type of interaction showing all residues interacting with GS-461203. Right: The 2D Protein-Ligand interactions Diagrams lasting more than 20% of the MDS.
Figure S5. The representative structure of the most dominant structural family for **A**: WT; **B**: T179A; **C**: S282T, **D**: M289L systems.
Figure S6. The least populated clusters for A: WT; B: T179A; C: S282T, D: M289L.
Figure S7. The RMSF values comparisons between WT and T179A (**A**), WT and S282T (**B**), and WT and M289L (**C**). The RMSF values of the C_α atoms for residues in WT (black), T179A (green), S282T (red), and M289L (blue) are shown, and the mutant positions are noted by red asterisks.
Figure S8. The RMSF values for atoms of GS-461203.
Figure S9. The RMSD of Protein Cα and ligand in T179A-CompA **(A)** and T179A-CompB **(B)** systems.
Figure S10. Protein-Ligand Interactions (**A:** T179A-CompA; **B:** T179A-CompB) recorded during MDS. Left: the histogram diagram and the fraction of the simulation for each type of interaction showing all residues interacting with GS-461203. Right: The 2D Protein-Ligand interactions Diagrams lasting more than 20% of the MDS.
Figure S11 The most dominant clusters for **A**: T179A-CompA; **B**: T179A-CompB systems.
Figure S12. The RMSF values comparisons between T179A, T179A-CompA, and T179A-CompB systems. The RMSF values of the C_α atoms for residues in T179A (black), T179A-CompA (green), and T179A-CompB (blue).
Figure S13. The RMSF values for atoms of GS-461203 in T179A, T179A-CompA, and T179A-CompB systems.
Figure S14. The ADME Properties of Sofosbuvir predicted by SwissAdme.
Figure S15. The ADME Properties of Sofosbuvir derivatives (F substituted by Cl) predicted by SwissAdme.
Figure S16. The ADME Properties of Sofosbuvir derivatives (F substituted by I) predicted by SwissAdme.
Figure S17. The ADME Properties of GS-461203 predicted by SwissAdme.
Figure S18. The ADME Properties of CompA predicted by SwissAdme.
Figure S19. The ADME Properties of CompB predicted by SwissAdme.

Table S1. The binding energies calculated for the last 50 ns of S282T system.

Systems	S282T
ΔG_{bind}	-41.3±5.4
$\Delta\Delta G_{bind}$	4.2
ΔE_{vdw}	2.4±12.1
$\Delta\Delta E_{vdw}$	8.4
ΔE_{ele}	-40.3±10.8
$\Delta\Delta E_{ele}$	5
ΔE_{lipo}	-3.4±0.9
$\Delta\Delta E_{lipo}$	0.9

Table S2. The binding energies calculated for the last 50 ns of each individual trajectory.

Systems	Run-1	Run-2
WT	-45.2±6.0	-45.8±5.6
T179	-35.0±5.9	-34.9±4.7
S282	-43.3±4.6	-39.2±5.5
M289	-58.0±6.4	-49.9±6.8

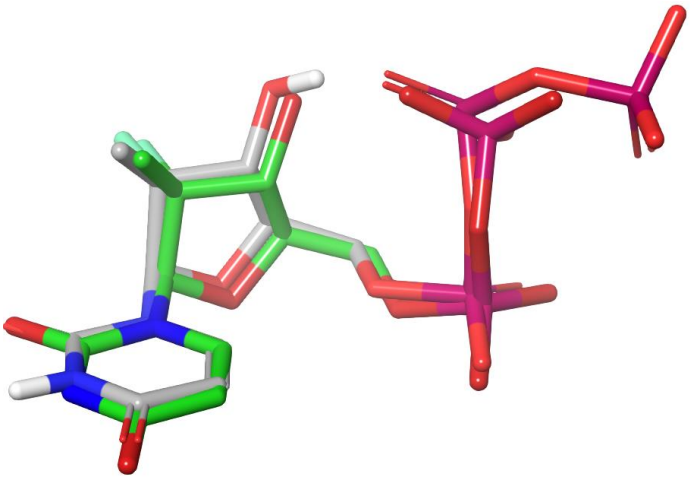

Figure S1. The docked GS-461203 (gray) and experimental poses of Sofosbuvir diphosphate (green).

A

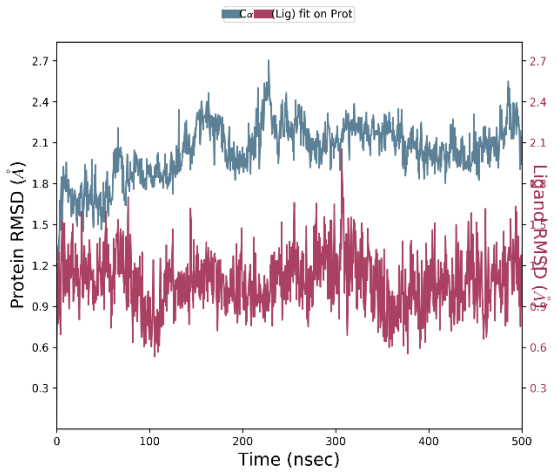
Cα (Lig) fit on Prot
Protein RMSD (Å)
Ligand RMSD (Å)
Time (nsec)

B

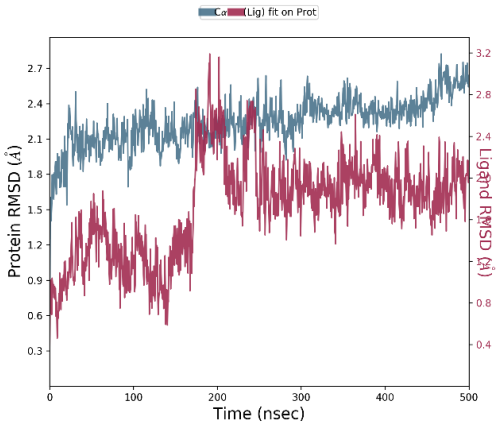
Cα (Lig) fit on Prot
Protein RMSD (Å)
Ligand RMSD (Å)
Time (nsec)

C

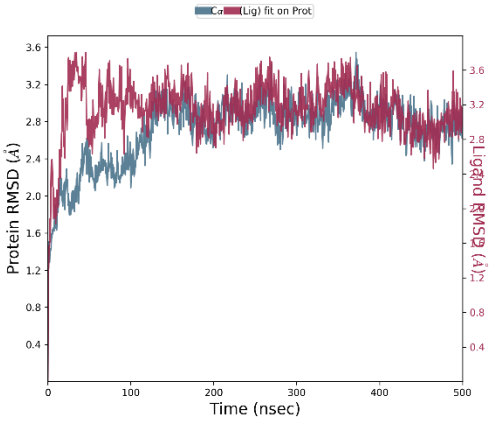
Cα (Lig) fit on Prot
Protein RMSD (Å)
Ligand RMSD (Å)
Time (nsec)

D

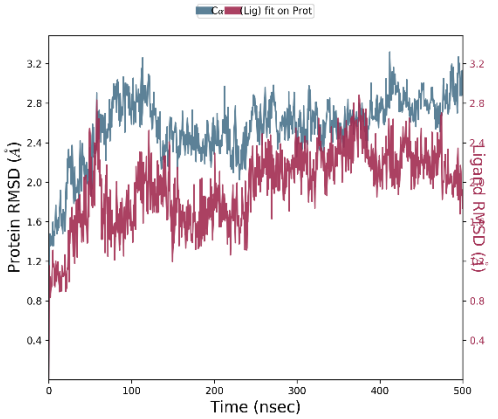
Cα (Lig) fit on Prot
Protein RMSD (Å)
Ligand RMSD (Å)
Time (nsec)

E

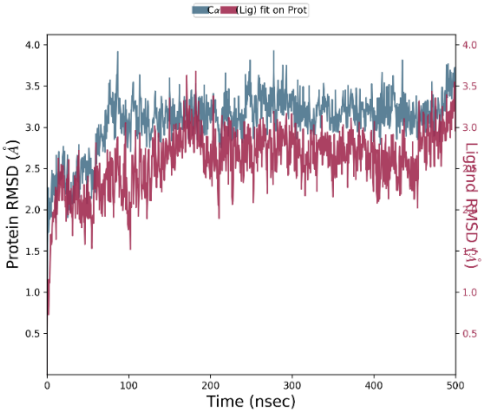
Cα (Lig) fit on Prot
Protein RMSD (Å)
Ligand RMSD (Å)
Time (nsec)

F

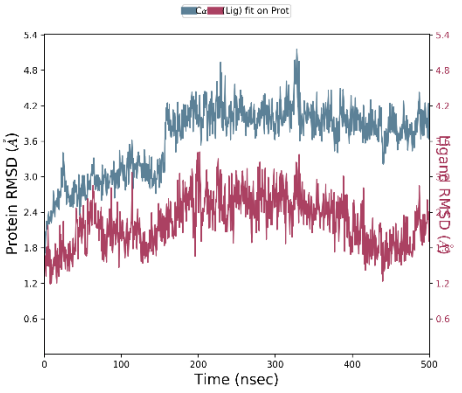
Cα (Lig) fit on Prot
Protein RMSD (Å)
Ligand RMSD (Å)
Time (nsec)

G

H

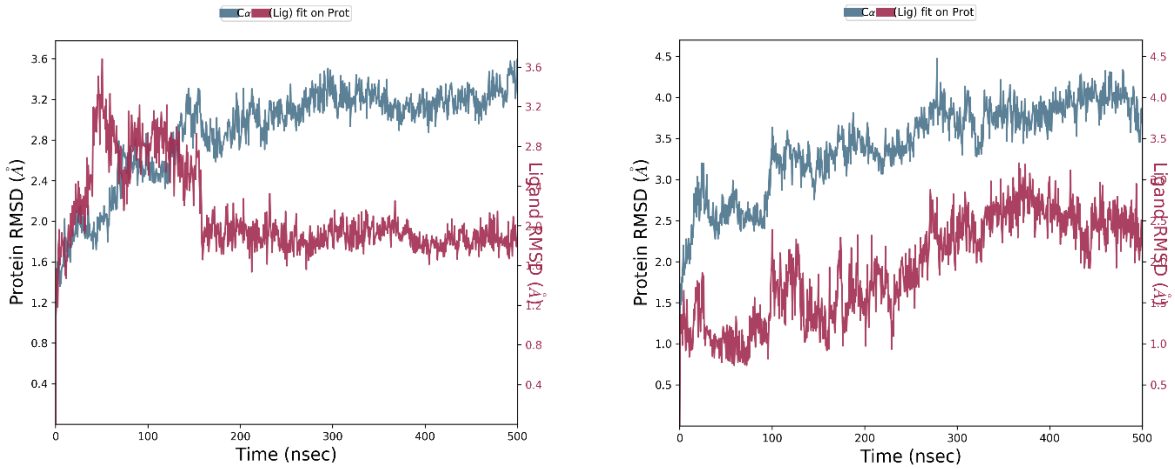

Figure S2. The RMSD of Protein Cα and ligand in WT run-1 (A), WT run-2 (B); T179A-run1 (C), T179A run-2 (D), S282T run-1 (E), S282T-run2 (F), M289L run-1 (G), and M289L run-2.

A

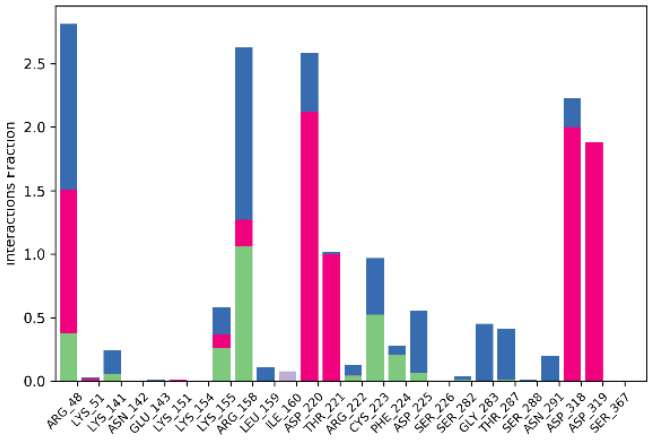

B

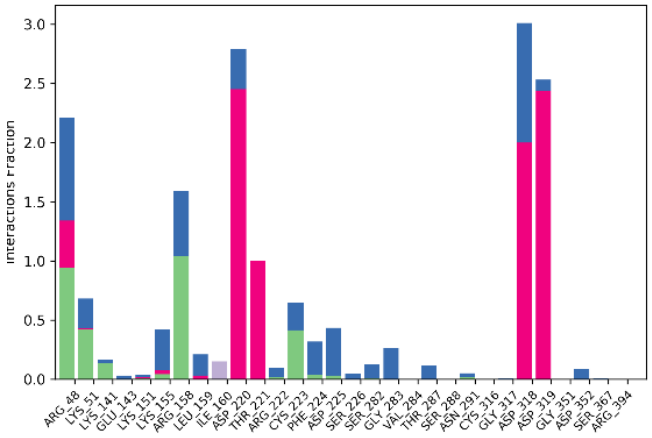

C

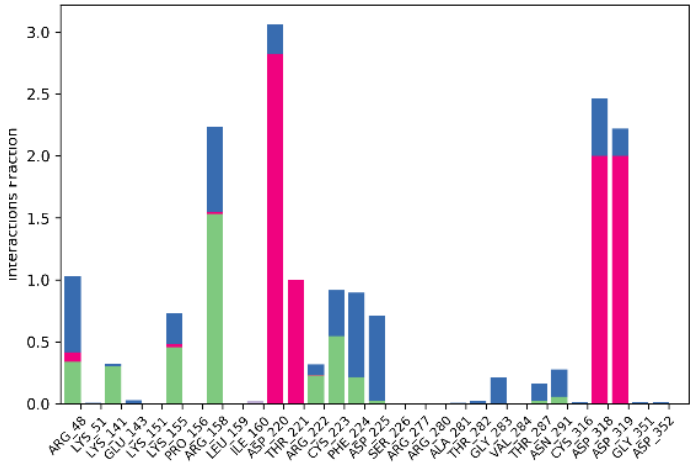

D

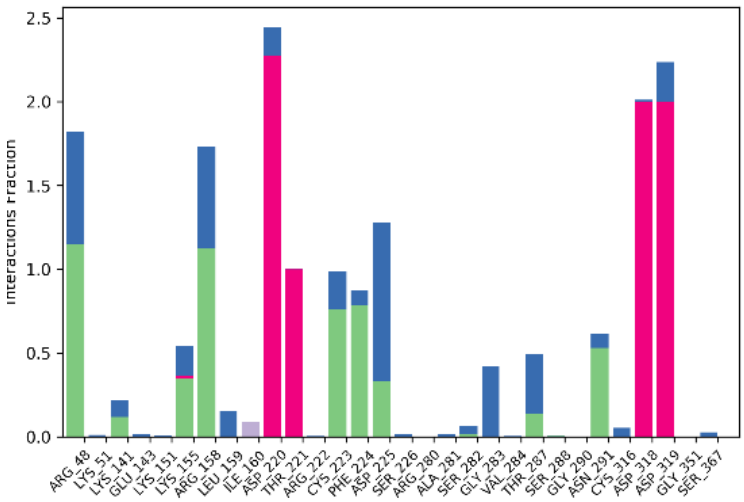

Figure S3. The histogram diagram and the fraction of the simulation for each type of interaction showing all residues interacting with GS-461203 (**A:** WT-GS-461203; **B:** T179A-GS-461203; **C:** S282T-GS-461203; **D:** M289L-GS-461203) recorded during MDS.

A

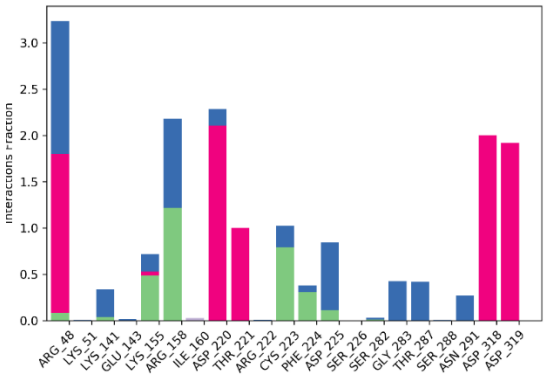
interactions fraction
3.0
2.5
2.0
1.5
1.0
0.5
0.0
ARG_48
LYS_51
LYS_141
GLU_143
LYS_155
ARG_158
ILE_160
ASP_220
THR_221
ARG_222
CYS_223
PHE_224
ASP_225
SER_226
SER_282
GLY_283
THR_287
SER_288
ASN_291
ASP_318
ASP_319

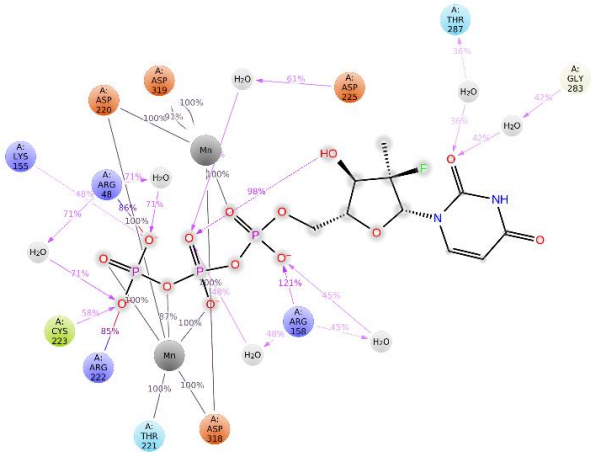
A: THR 287
A: GLY 283
A: ASP 319
A: ASP 220
A: ASP 225
A: LYS 155
A: ARG 48
A: CYS 223
A: ARG 222
A: ARG 158
A: THR 221
A: ASP 318
Mn
H₂O
HO
F
NH
O
N
P

B

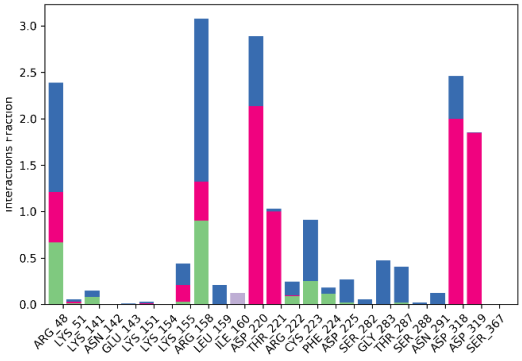
interactions fraction
3.0
2.5
2.0
1.5
1.0
0.5
0.0
ARG_48
LYS_51
LYS_141
ASN_142
GLU_143
LYS_151
LYS_154
LYS_155
ARG_158
LEU_159
ILE_160
ASP_220
THR_221
ARG_222
CYS_223
PHE_224
ASP_225
SER_282
GLY_283
THR_287
SER_288
ASN_291
ASP_318
ASP_319
SER_367

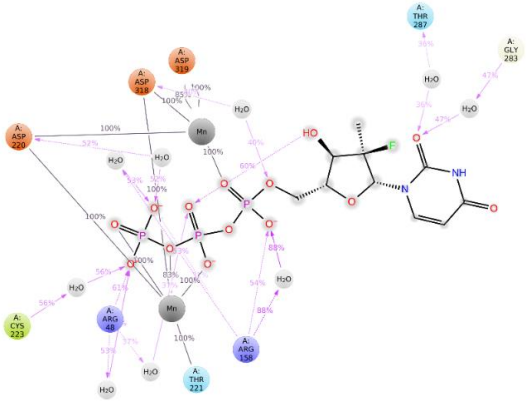
A: THR 287
A: GLY 283
A: ASP 319
A: ASP 318
A: ASP 220
A: CYS 223
A: ARG 48
A: ARG 158
A: THR 221
Mn
H₂O
HO
F
NH
O
N
P

C

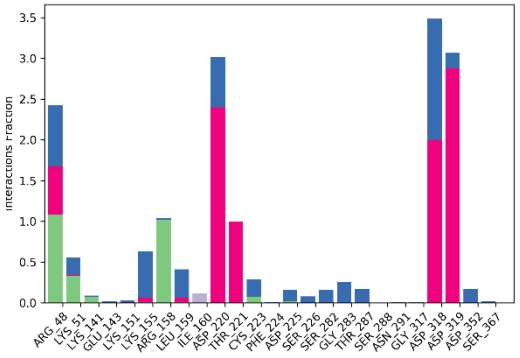
interactions fraction
3.5
3.0
2.5
2.0
1.5
1.0
0.5
0.0
ARG_48
LYS_51
LYS_141
GLU_143
LYS_151
LYS_155
ARG_158
LEU_159
ILE_160
ASP_220
THR_221
CYS_223
PHE_224
ASP_225
SER_226
SER_282
GLY_283
THR_287
SER_288
ASN_291
GLY_317
ASP_318
ASP_319
ASP_352
SER_367

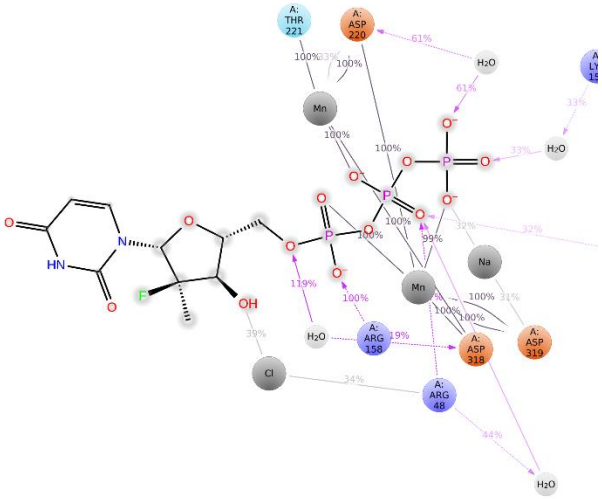
A: THR 221
A: ASP 220
A: ASP 319
A: ARG 158
A: ARG 48
A: ASP 318
Mn
Na
Cl
H₂O
HN
O
N
P
F
OH

D

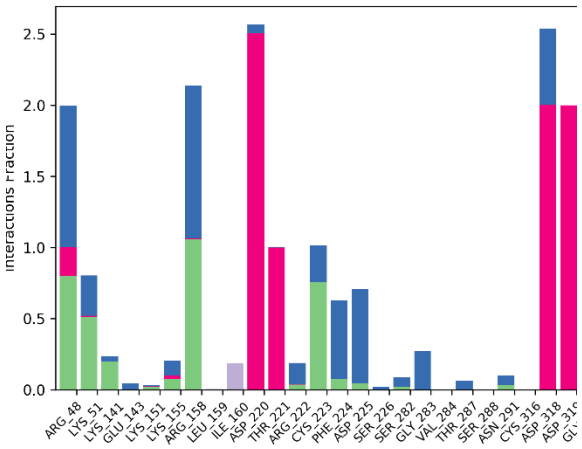
interactions fraction
2.5
2.0
1.5
1.0
0.5
0.0
ARG_48
LYS_51
LYS_141
GLU_143
LYS_151
LYS_155
ARG_158
LEU_159
ILE_160
ASP_220
THR_221
ARG_222
CYS_223
PHE_224
ASP_225
SER_226
SER_282
GLY_283
VAL_284
THR_287
SER_288
ASN_291
CYS_316
ASP_318

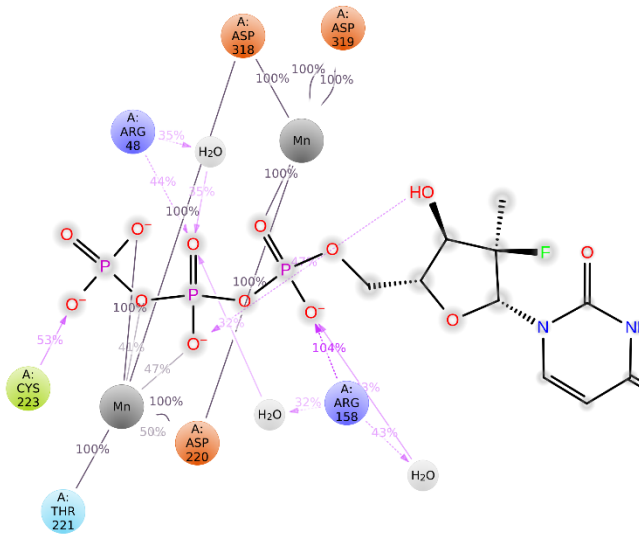
A: ASP 318
A: ASP 319
A: ARG 48
A: CYS 223
A: ASP 220
A: ARG 158
A: THR 221
Mn
H2O
HO
F
O
N
NH

E

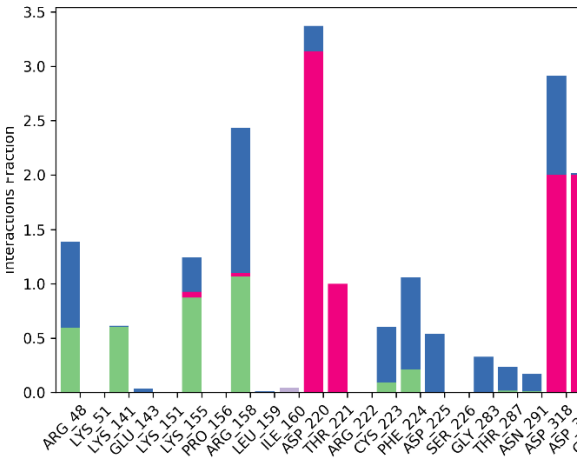
interactions fraction
3.5
3.0
2.5
2.0
1.5
1.0
0.5
0.0
ARG_48
LYS_51
LYS_141
GLU_143
LYS_151
LYS_155
PRO_156
ARG_158
LEU_159
ILE_160
ASP_220
THR_221
ARG_222
CYS_223
PHE_224
ASP_225
SER_226
GLY_283
THR_287
ASN_291
ASP_318

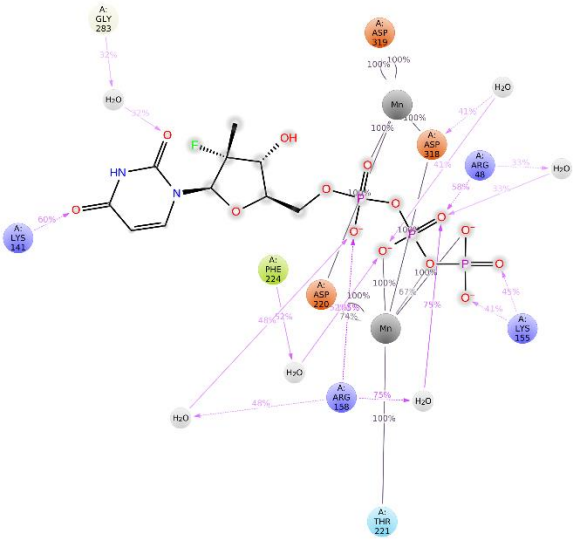
A: GLY 283
A: ASP 319
A: ARG 48
A: LYS 141
A: PHE 224
A: ASP 220
A: ARG 158
A: LYS 155
A: THR 221
Mn
H2O
OH
F
HN
O
N
P

F

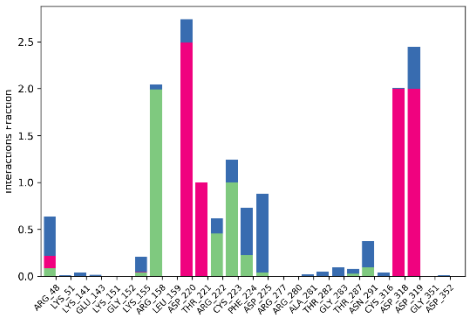
interactions fraction
2.5
2.0
1.5
1.0
0.5
0.0

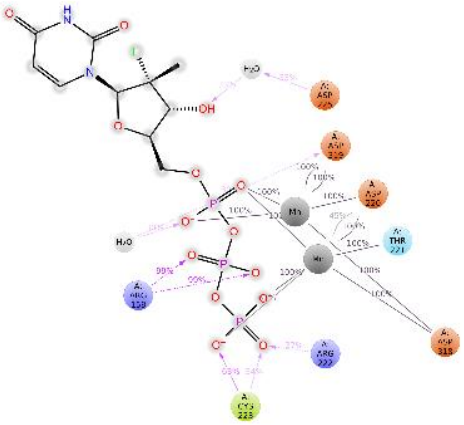
OH
F
O
N
H2O
Mn
P

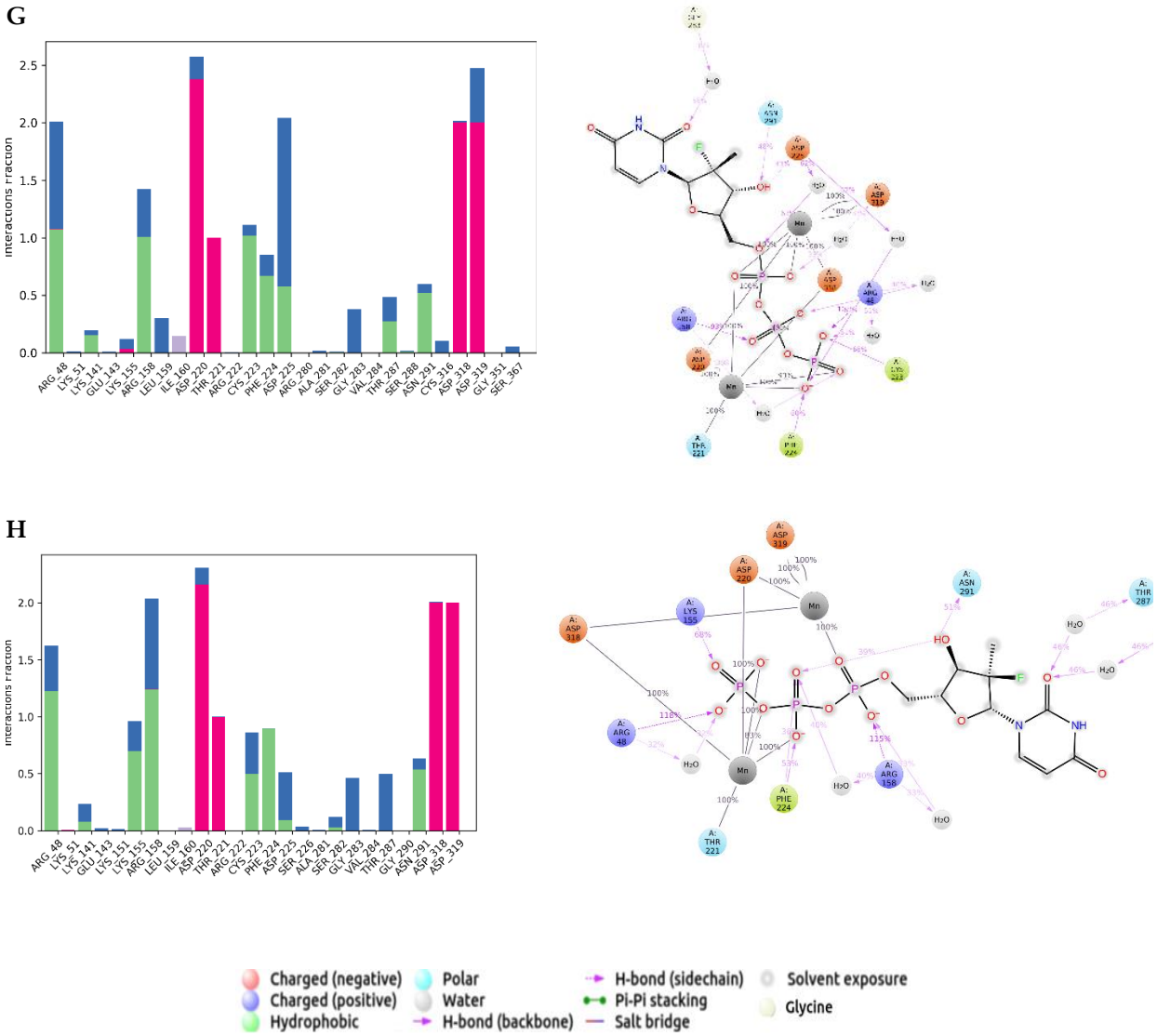

Figure S4. Protein-Ligand Interactions **A:** WT-GS-461203-run1; **B:** WT-GS-461203-run2; **C:** T179A-GS-461203-run1; **D:** T179A-GS-461203-run2; **E:** S282T-GS-461203-run1; **F:** S282T-GS-461203-run2; **G:** M289L-GS-461203-run1; **H:** M289L-GS-461203-run2, recorded during MDS. Left: the histogram diagram and the fraction of the simulation for each type of interaction showing all residues interacting with GS-461203. Right: The 2D Protein-Ligand interactions Diagrams lasting more than 20% of the MDS.

A

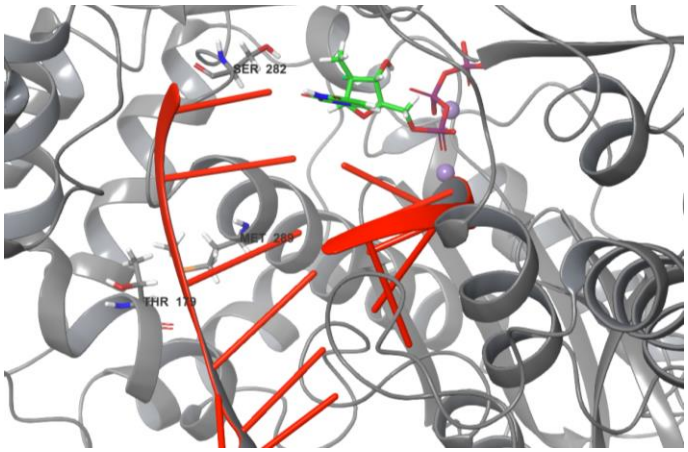
SER 282
MET 289
THR 179

B

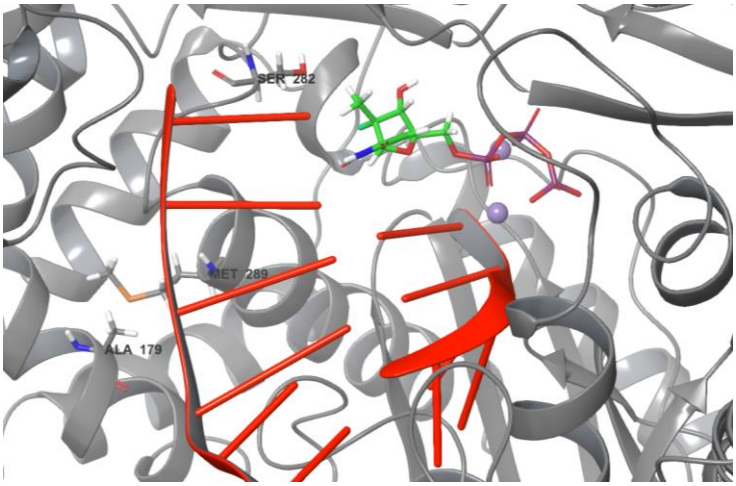
SER 282
MET 289
ALA 179

C

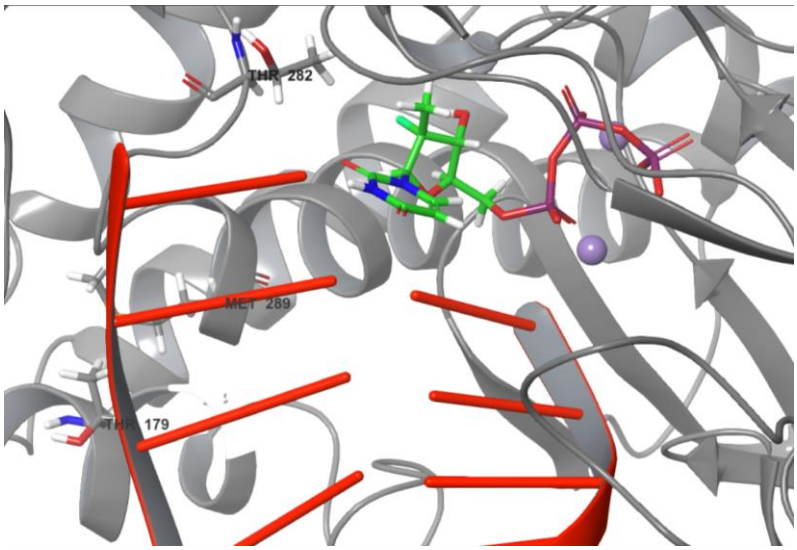
THR 282
MET 289
THR 179

D

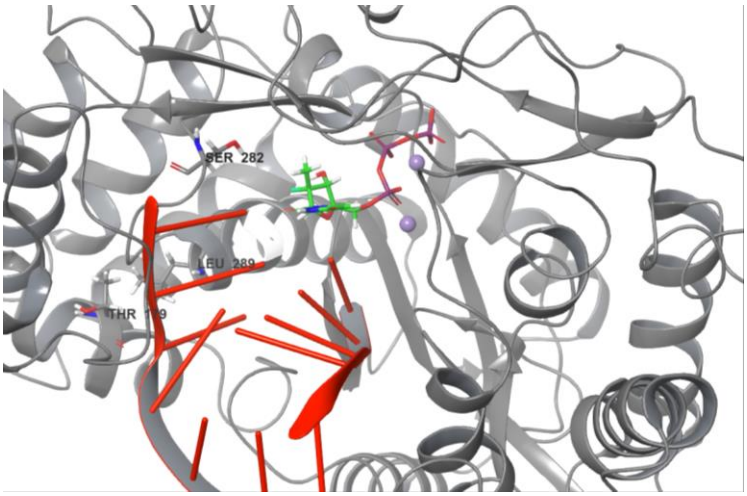

Figure S5. The representative structure of the most dominant structural family for **A**: WT; **B**: T179A; **C**: S282T, **D**: M289L systems.

A

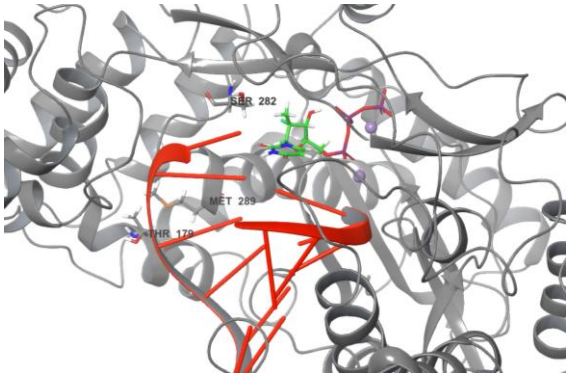

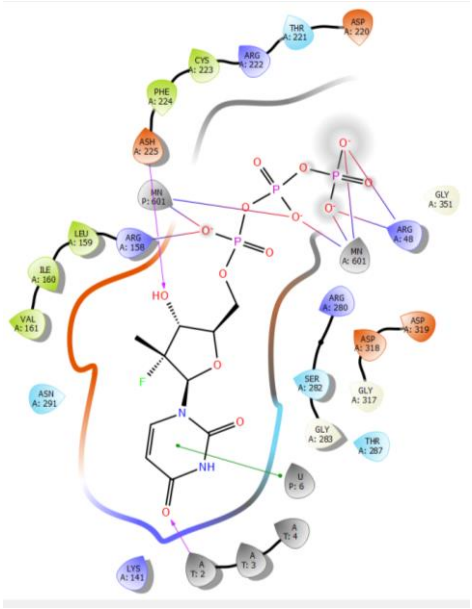

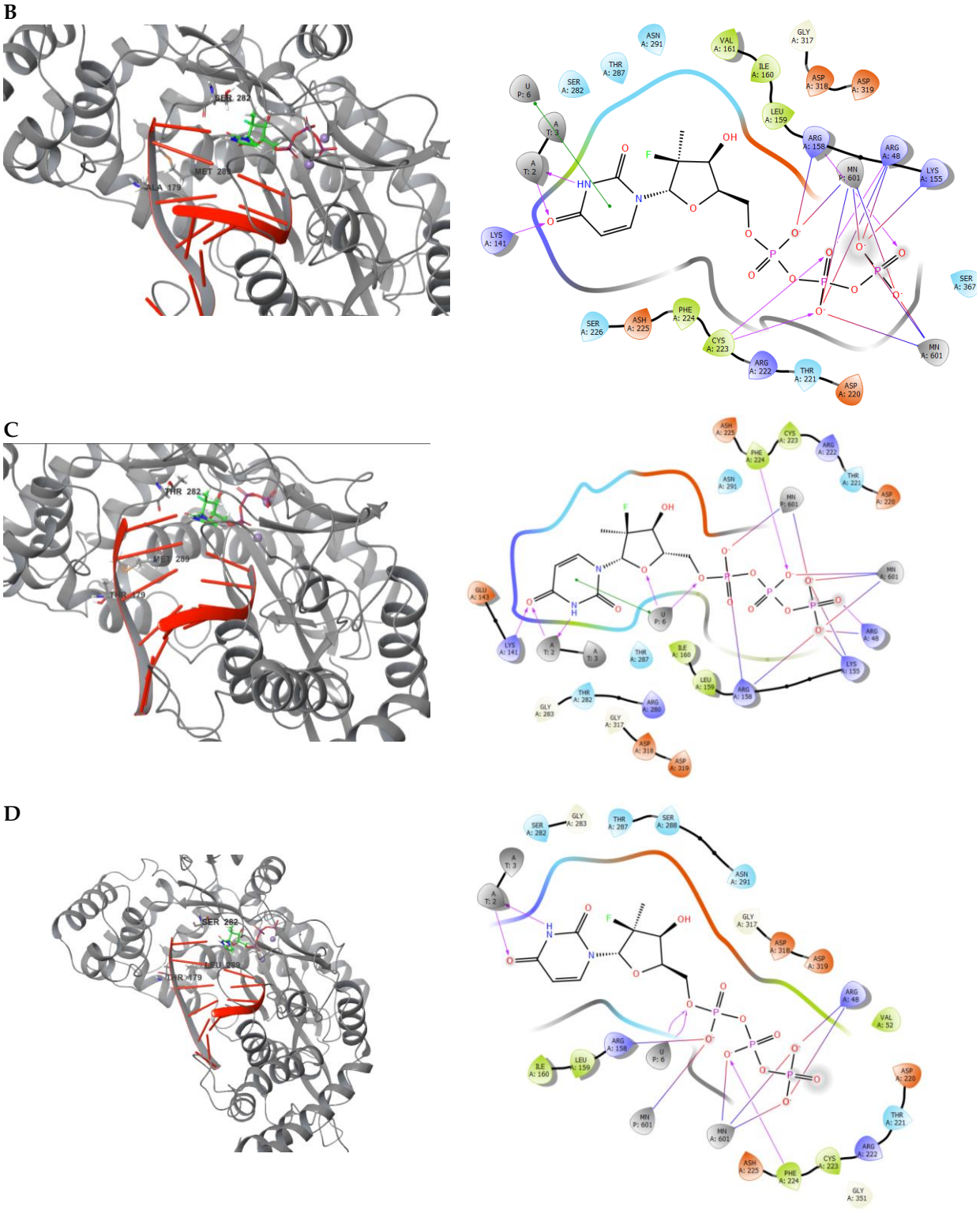

Figure S6. The least populated clusters for A: WT; B: T179A; C: S282T, D: M289L.

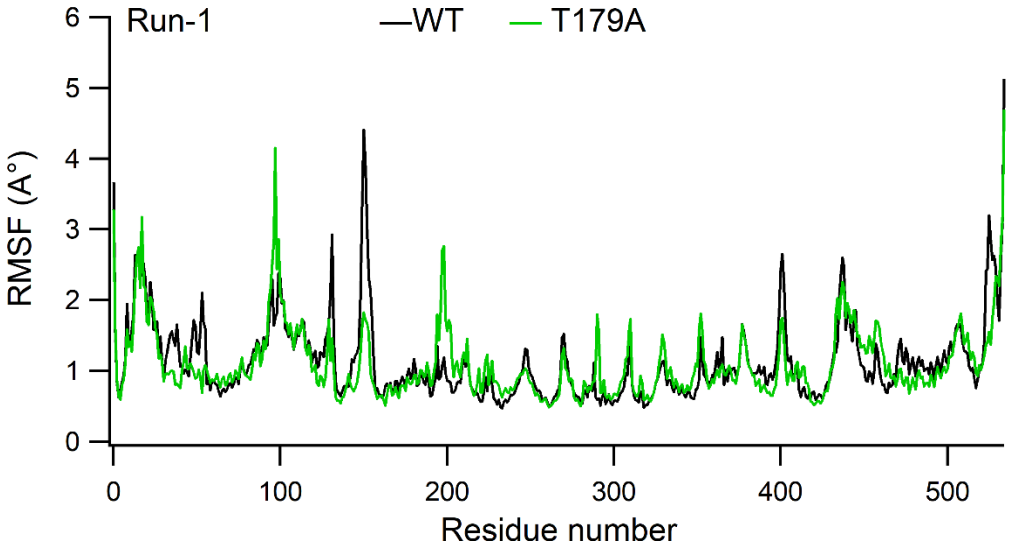
Run-1
—WT
— T179A
RMSF (A°)
0
1
2
3
4
5
6
0
100
200
300
400
500
Residue number

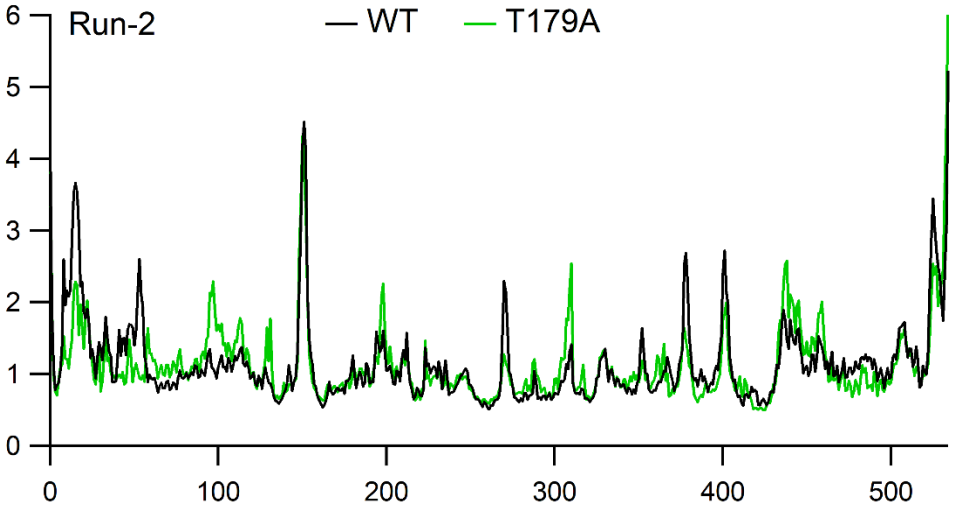
Run-2
— WT
— T179A
0
1
2
3
4
5
6
0
100
200
300
400
500

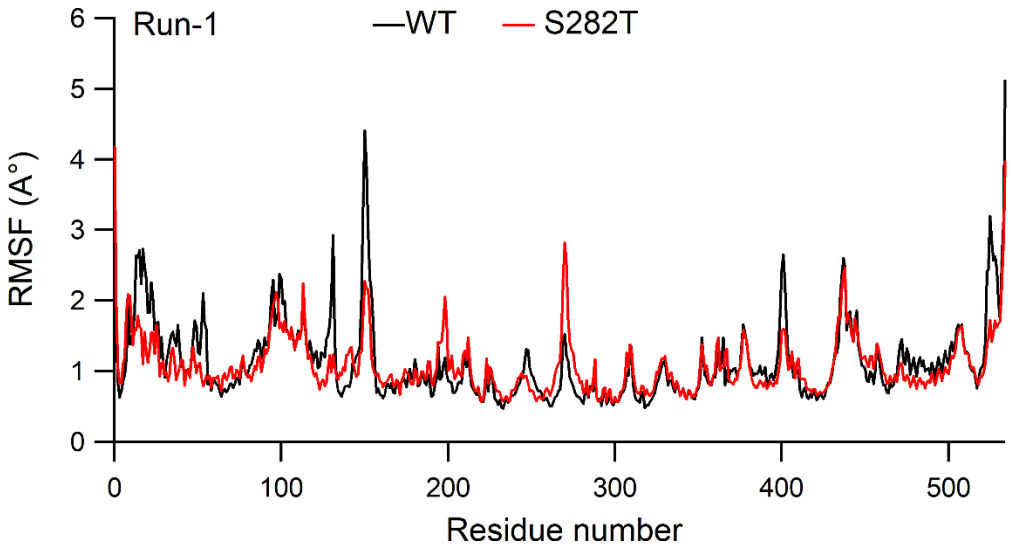
Run-1
—WT
— S282T
RMSF (A°)
0
1
2
3
4
5
6
0
100
200
300
400
500
Residue number

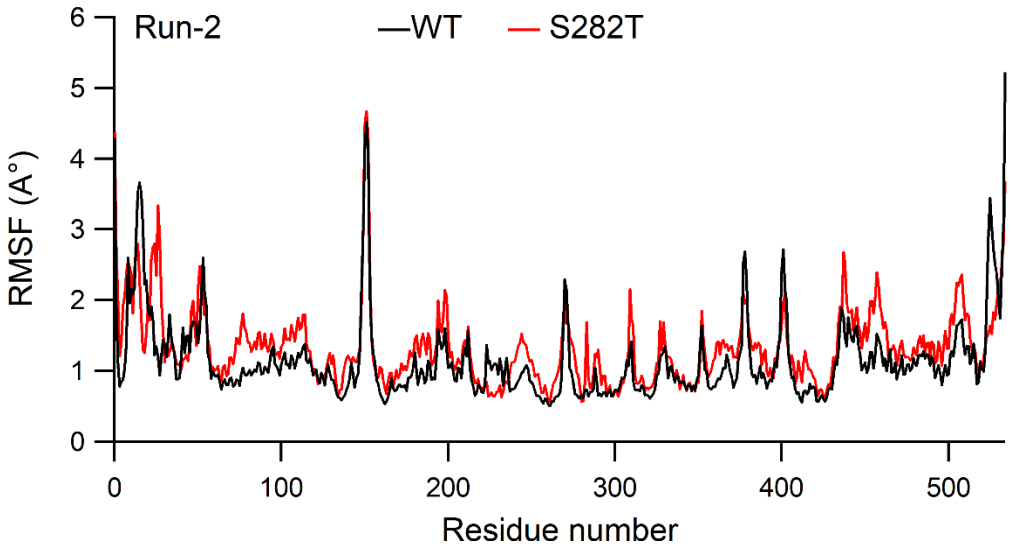
Run-2
—WT
— S282T
RMSF (A°)
0
1
2
3
4
5
6
0
100
200
300
400
500
Residue number

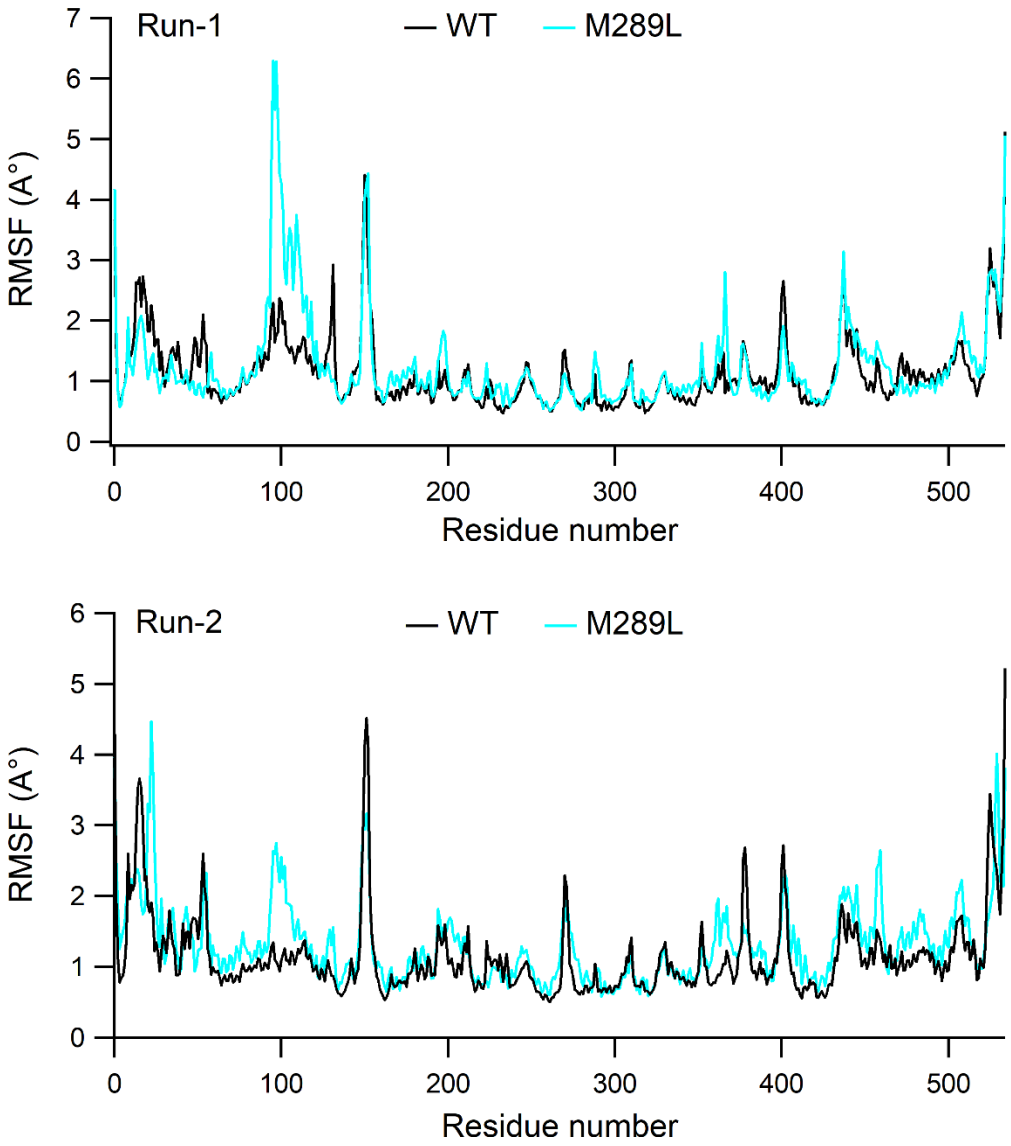

Figure S7. The RMSF values comparisons between WT and T179A (**A**), WT and S282T (**B**), and WT and M289L (**C**). The RMSF values of the C_α atoms for residues in WT (black), T179A (green), S282T (red), and M289L (blue) are shown, and the mutant positions are noted by red asterisks.

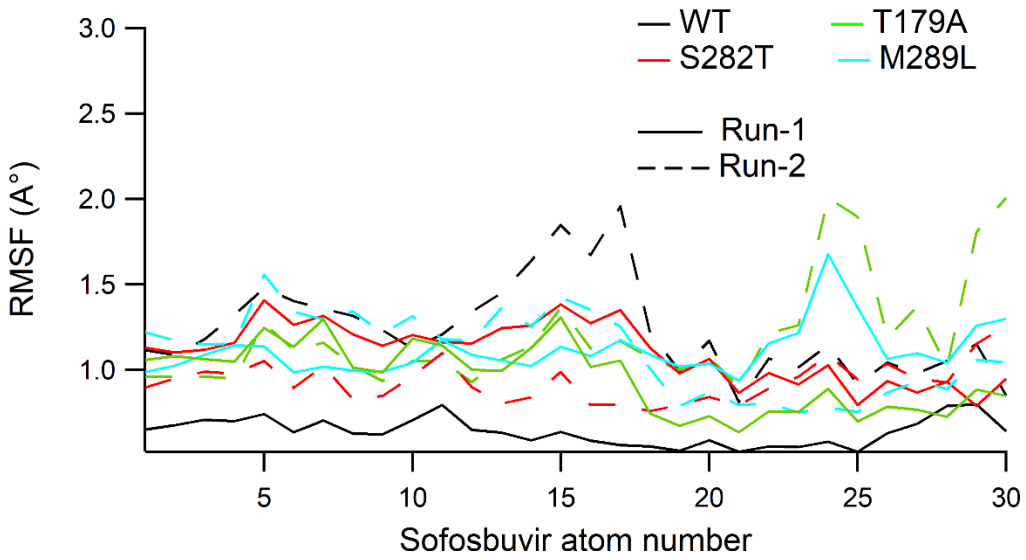

Figure S8. The RMSF values for atoms of GS-461203.

A

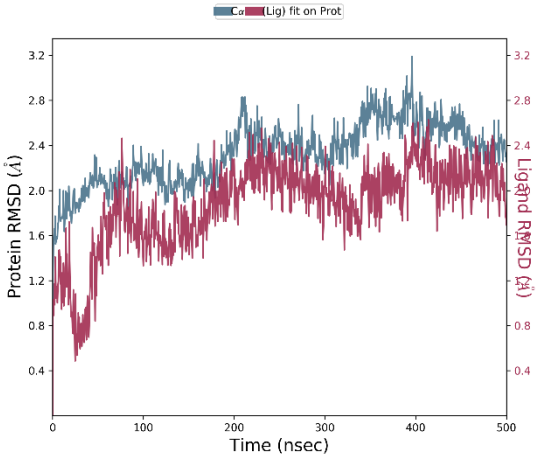

B

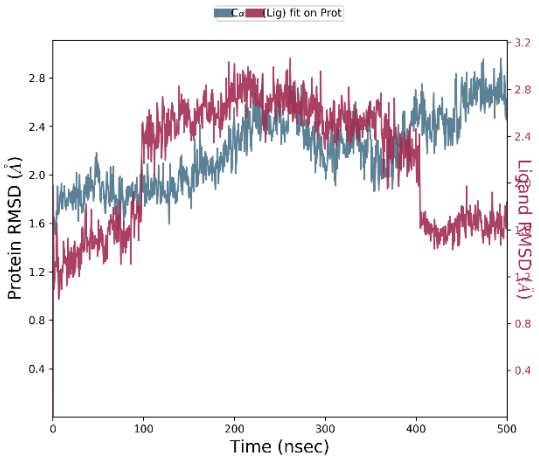

Figure S9. The RMSD of Protein C*α* and ligand in T179A-CompA **(A)** and T179A-CompB **(B)** systems.

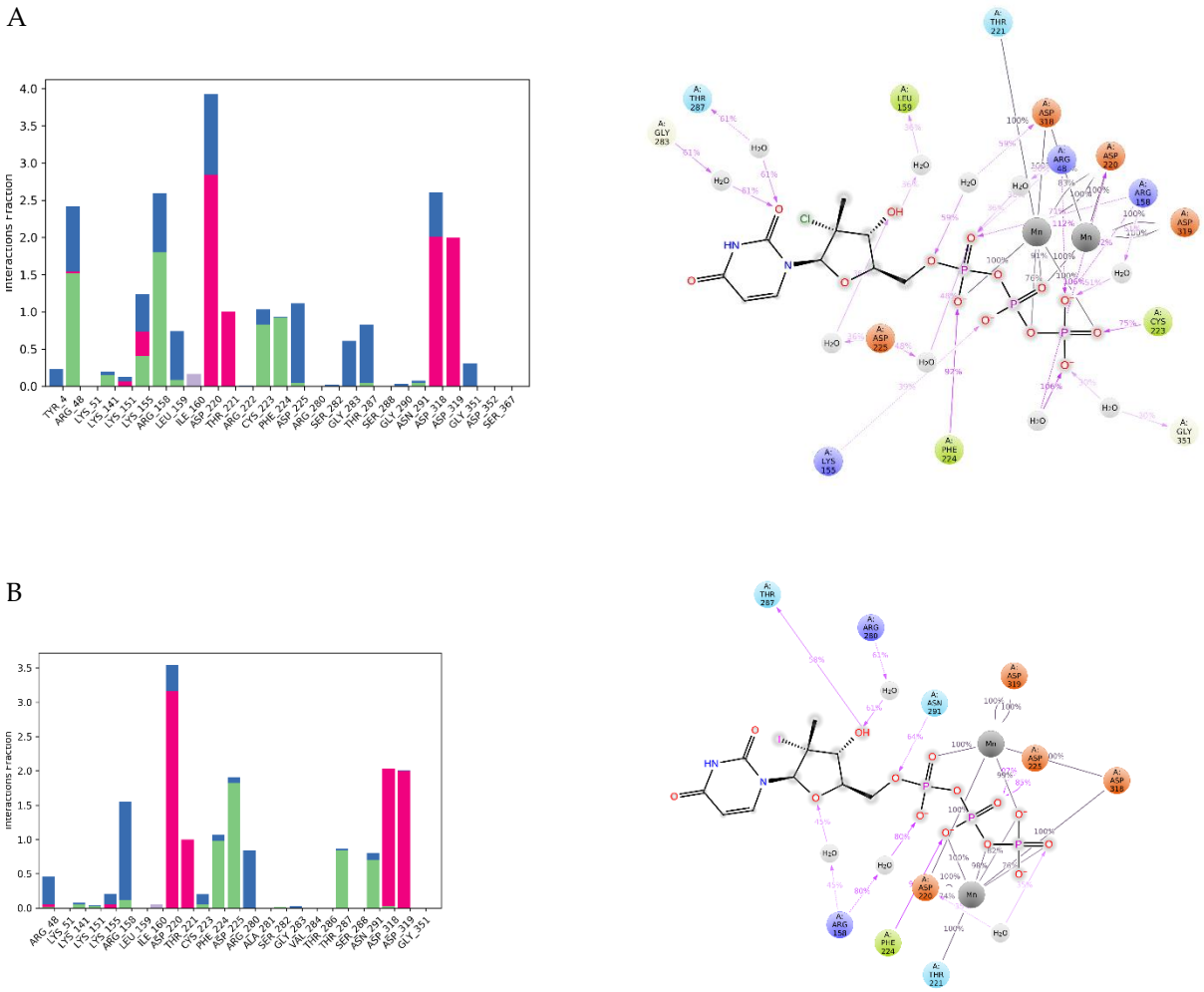

Figure S10. Protein-Ligand Interactions (**A:** T179A-CompA; **B:** T179A-CompB) recorded during MDS. Left: the histogram diagram and the fraction of the simulation for each type of interaction showing all residues interacting with GS-461203. Right: The 2D Protein-Ligand interactions Diagrams lasting more than 20% of the MDS.

A

B

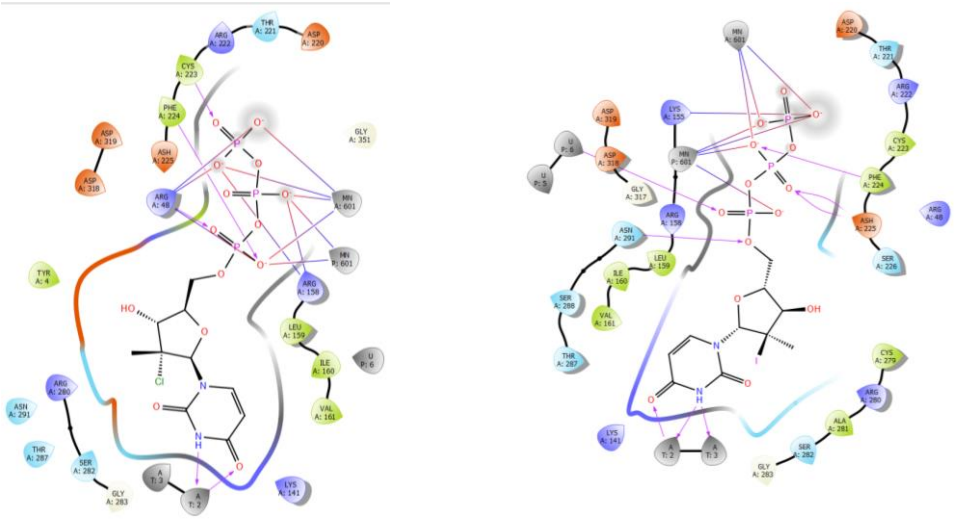

Figure S11. The most dominant clusters for **A**: T179A-CompA; **B**: T179A-CompB systems.

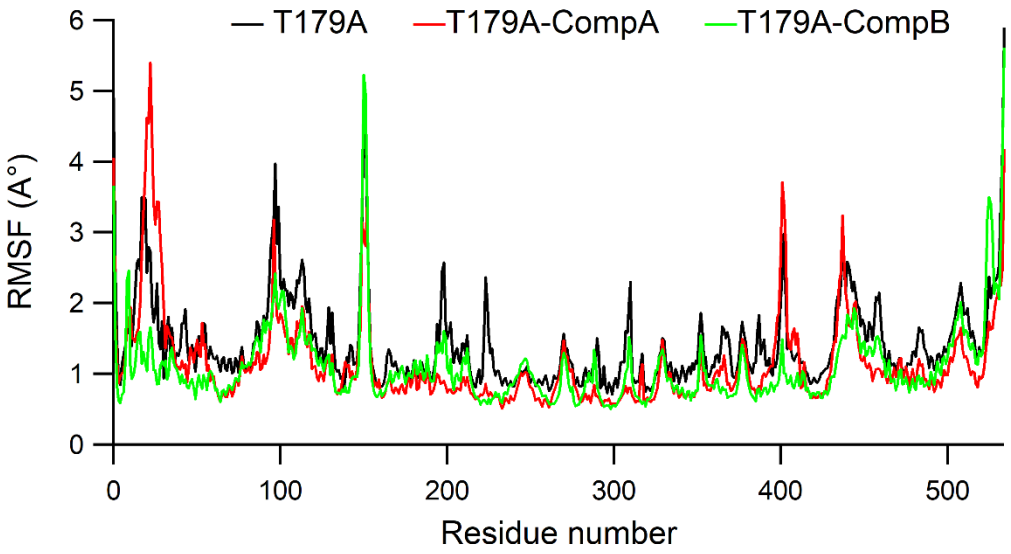

Figure S12. The RMSF values comparisons between T179A, T179A-CompA, and T179A-CompB systems. The RMSF values of the C_α atoms for residues in T179A (black), T179A-CompA (green), and T179A-CompB (blue).

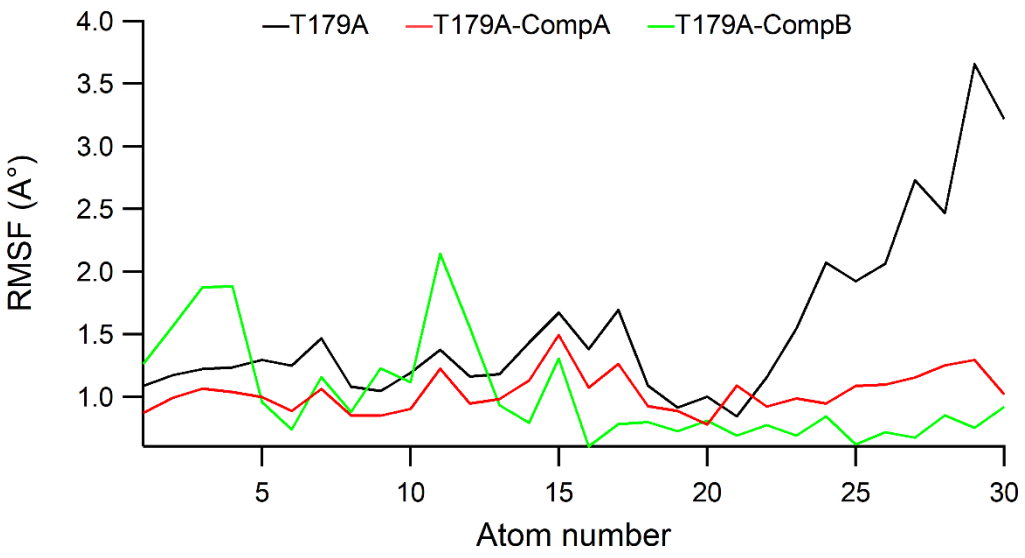

Figure S13. The RMSF values for atoms of GS-461203 in T179A, T179A-CompA, and T179A-CompB systems.

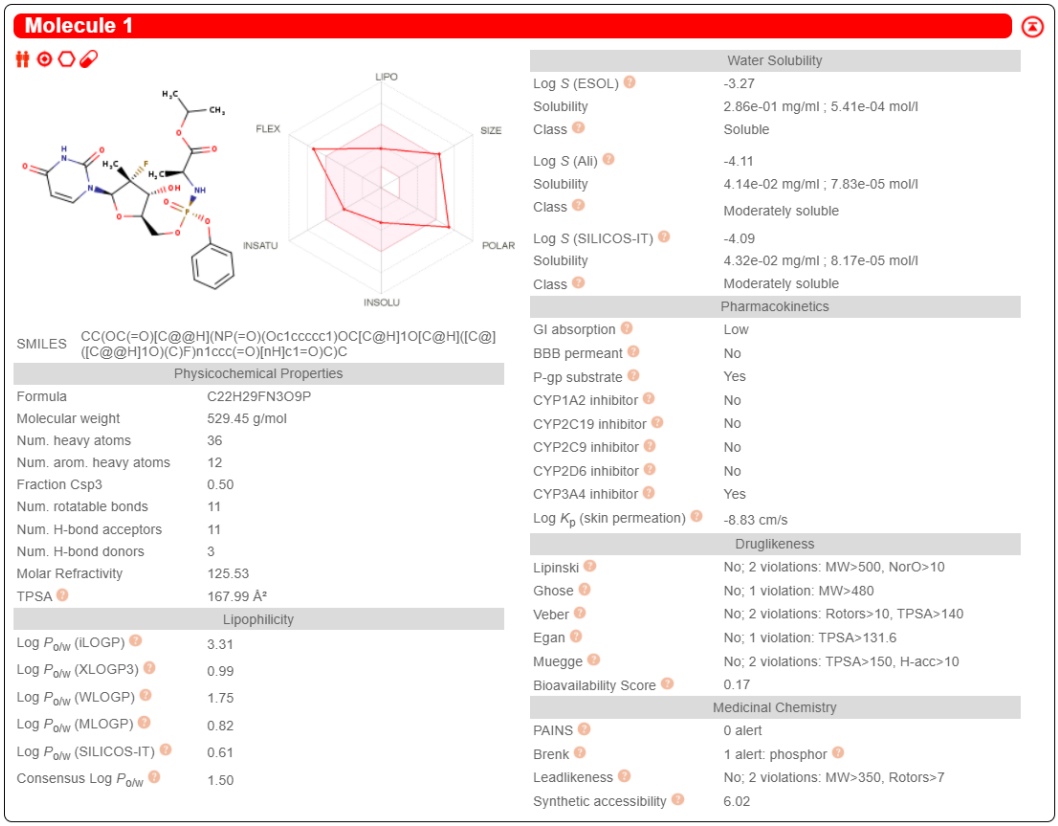

Figure S14. The ADME Properties of Sofosbuvir predicted by SwissAdme.

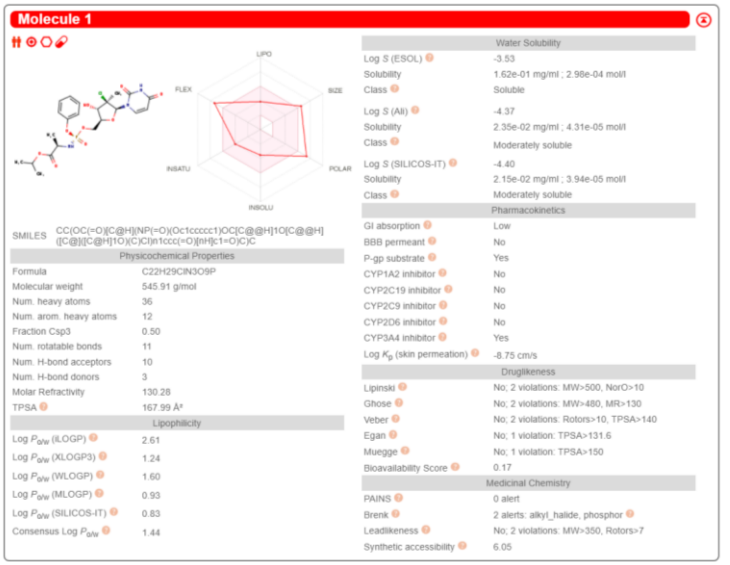

Figure S15. The ADME Properties of Sofosbuvir derivatives (F substituted by Cl) predicted by SwissAdme.

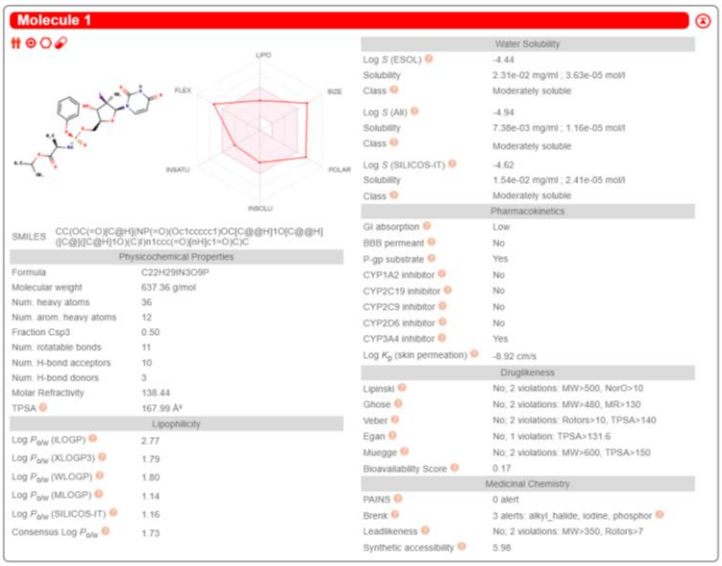

Figure S16. The ADME Properties of Sofosbuvir derivatives (F substituted by I) predicted by SwissAdme.

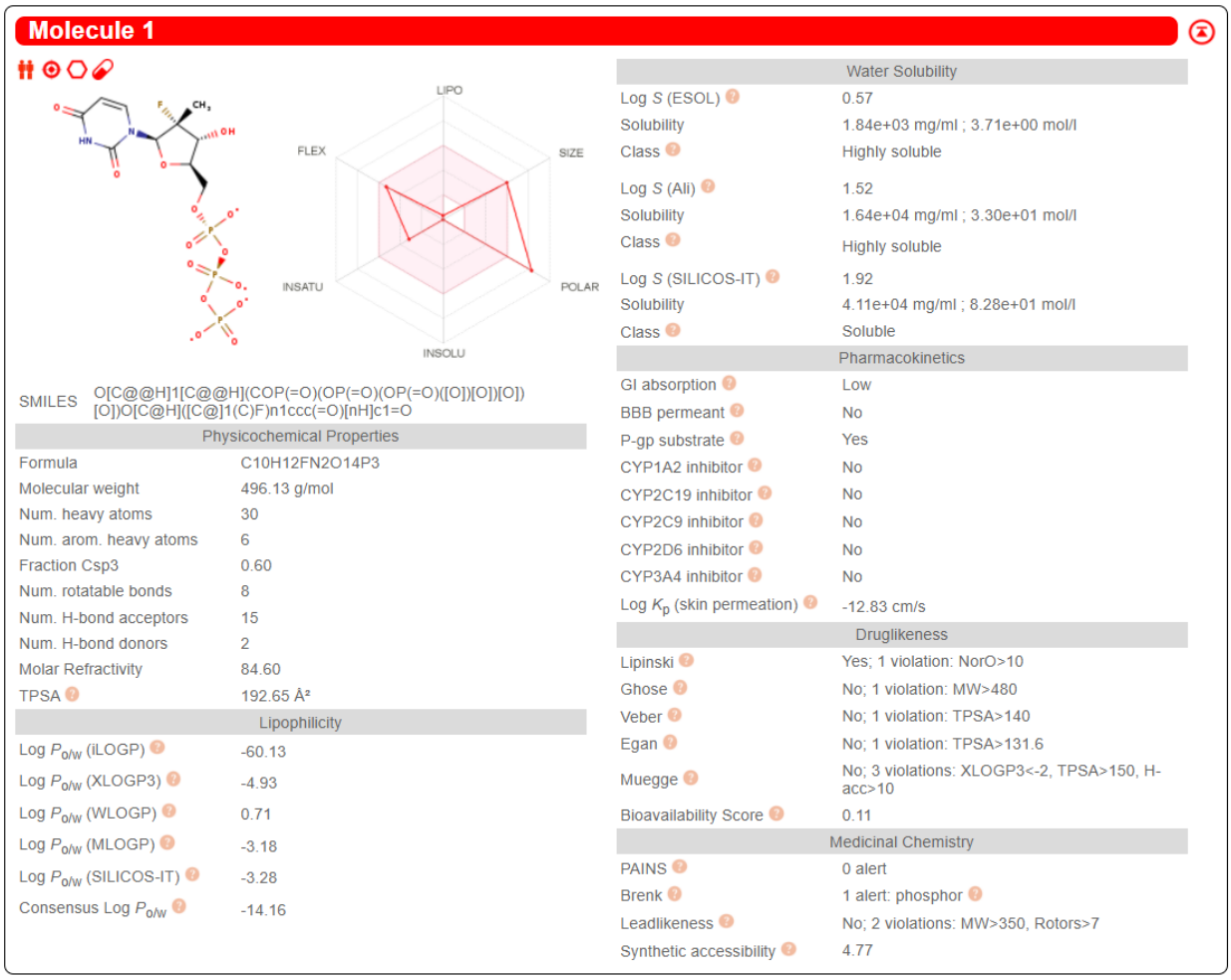

Figure S17. The ADME Properties of GS-461203 predicted by SwissAdme.

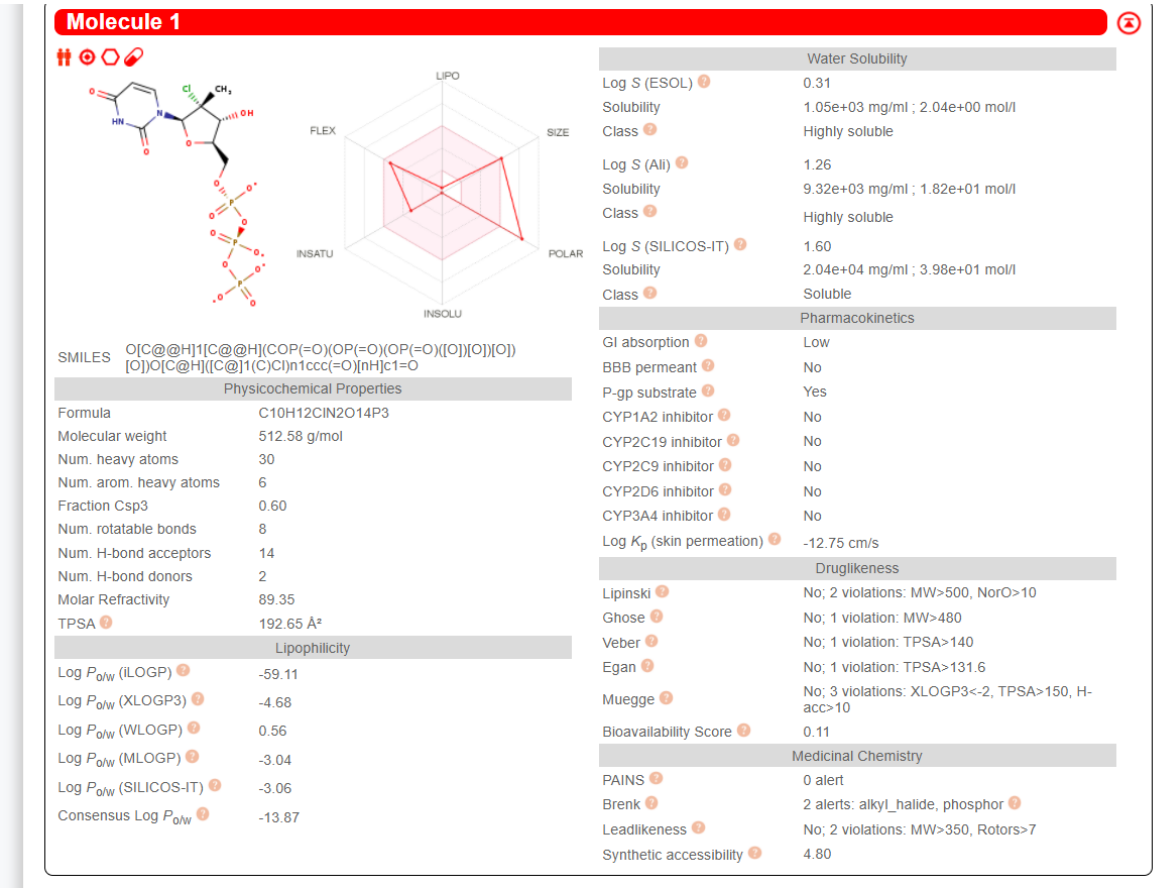

Figure S18. The ADME Properties of CompA predicted by SwissAdme.

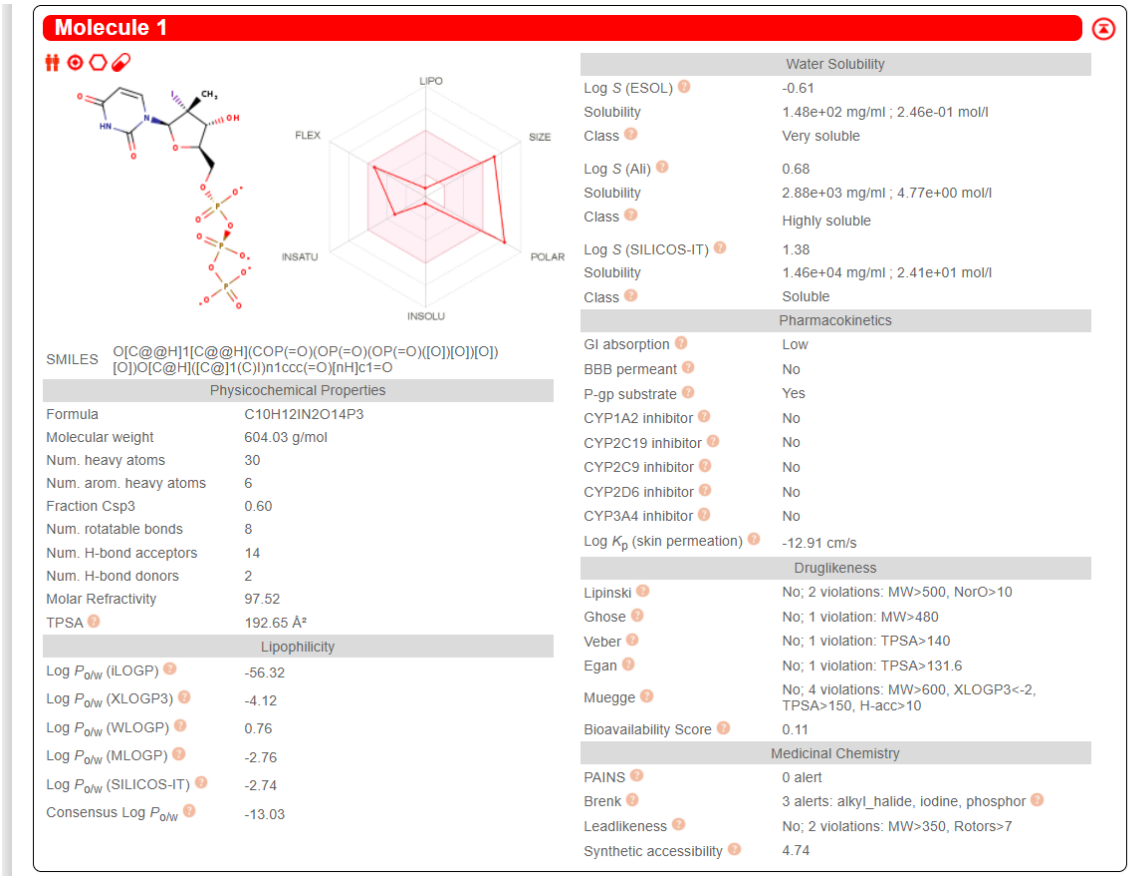

Figure S19. The ADME Properties of CompB predicted by SwissAdme.